

## Aerodynamic advantages of upside down take-off for aerial dispersal in *Tetranychus* spider mites

Mh. Osakabe · H. Isobe · A. Kasai · R. Masuda · S. Kubota · M. Umeda

Received: 1 October 2007 / Accepted: 13 March 2008 / Published online: 8 April 2008  
© Springer Science+Business Media B.V. 2008

**Abstract** Aerial dispersal may be important for redistribution of spider mites into new habitats. Evidence for behavioral control of aerial take-off has been well documented for *Tetranychus urticae* Koch. Before aerial dispersal they exhibit the aerial take-off posture that involves lifting the forelegs upright and raising the forebody. However, whether the aerial take-off posture functions to increase drag has remained unclear. The objectives of this study were to clarify: (i) aerodynamic effects of the aerial take-off posture; and (ii) actual aerial take-off behavior in *T. urticae*. To evaluate the aerodynamic forces experienced by grounded spider mites in different postures, we constructed three-dimensional models of *T. urticae*, exhibiting the aerial take-off posture and the normal posture, using computer graphics. We found that the aerial take-off posture was effective in receiving greater rearward forces from wind rather than upward forces. As a result, aerial take-off from a horizontal platform is unlikely. Instead, inverted departure surfaces, e.g., lower leaf surfaces, with inclines are likely to be effective sites for take-off. Laboratory experiments and field observations indicated that the mites preferentially adopted such a position for orientation and take-off. Our findings provided a rationale for the take-off behavior of *Tetranychus* spider mites.

**Keywords** Aerodynamic forces · Wind-borne dispersal · Aerial take-off posture · Tetranychidae · *Tetranychus urticae* Koch

---

Mh. Osakabe (✉) · A. Kasai  
Laboratory of Ecological Information, Graduate School of Agriculture, Kyoto University,  
Kyoto 606-8502, Japan  
e-mail: mhosaka@kais.kyoto-u.ac.jp

H. Isobe · R. Masuda · M. Umeda  
Laboratory of Field Robotics, Graduate School of Agriculture, Kyoto University,  
Kyoto 606-8502, Japan

S. Kubota  
Fuji Branch, Shizuoka Tea Experiment Station, Fuji, Shizuoka 417-0862, Japan

*Present Address:*

S. Kubota  
Deciduous Fruit Tree Branch, Shizuoka Prefectural Citrus Experiment Station, Hamamatsu,  
Shizuoka 431-2102, Japan

## Introduction

Aerial dispersal behavior may have evolved as a means for large-scale movement from one unfavorable habitat to another, potentially better habitat, in many flightless arthropods. Small wingless arthropods are sometimes considered to be detached accidentally from their host plants. However, their behavior suggests that they are drawn actively into the air stream. Crawlers of the ice plant scale, *Pulviniella mesembryanthemi* (Vallot) (Homoptera: Coccoidea), exploit boundary layer velocity gradients by exhibiting an aerial take-off posture that involves lifting the prothoracic legs and forebody and standing on the meso- and metathoracic legs (Washburn and Washburn 1984). Such aerial take-off posture has also been observed in other scale insects (Stephens and Aylor 1978; Gullan and Kosztarab 1997), phytoseiid mites (Johnson and Croft 1976; Hoy 1982; Croft and Jung 2001), which are selective predators of *Tetranychus* spider mites (McMurtry and Croft 1997), except for *Phytoseiulus persimilis* Athias-Henriot (Acari: Phytoseiidae) (Sabelis and Afman 1994), and herbivorous eriophyid mites (Duffner et al. 2001). These behaviors may efficiently increase drag force; if they do not stand up, they may be embedded in the laminar boundary layer formed at the leading edge of the plant substrate (Washburn and Washburn 1984; Jung 2001). In addition, Sabelis and Afman (1994) documented behavioral control in that volatile chemicals (synomones) from a plant damaged by spider mite feeding suppressed aerial take-off of the specialist phytoseiid mite, *P. persimilis*.

For spider mites in unstable habitats, aerial dispersal is also likely to be an important event for redistribution into new habitats (Mitchell 1973; Brandenburg and Kennedy 1982; Boykin and Campbell 1984; Smitley and Kennedy 1988; Grafton-Cardwell et al. 1991; Lawson et al. 1996). The two-spotted spider mite, *Tetranychus urticae* Koch (Acari: Tetranychidae), exhibits an aerial take-off behavior that involves lifting the first legs upright and raising the forebody (Smitley and Kennedy 1985; Margolies 1987; Li and Margolies 1993a). Bell et al. (2005) reported incorporation of wind-borne dispersal by *T. urticae* into a means of ballooning. Indeed, ballooning behavior using threads has been observed in many spider mites. Examples include the citrus red mite, *Panonychus citri* (McGregor), the avocado brown mite, *Oligonychus punicae* (Hirst), the tea red spider mite, *Oligonychus coffeae* (Nietner), and the six-spotted mite, *Eotetranychus sexmaculatus* (Riley) (Acari: Tetranychidae; Fleschner et al. 1956; Das 1959). However, despite its complicated web production (Saito 1983), there is no evidence that *T. urticae* uses threads when it takes off (Fleschner et al. 1956; Hussey and Parr 1963; Boykin and Campbell 1984; Smitley and Kennedy 1985; Margolies 1987).

*Tetranychus urticae* and the Banks grass mite, *Oligonychus pratensis* (Banks) (Acari: Tetranychidae), exhibit aerial take-off behavior only in the presence of wind and light, but these stimuli alone are not sufficient to elicit the response if the microhabitat is satisfied (Margolies 1987). Food shortage and desiccation increase the number of individuals exhibiting such active aerial take-off behaviors (Boykin and Campbell 1984; Smitley and Kennedy 1985; Margolies 1987). Because of their vigorous reproduction, spider mites cause deterioration of leaves and plants, with the result that they experience both food shortages and desiccation (Sances et al. 1979; De Angelis et al. 1982). Although individuals in every life stage except adult males exhibit aerial take-off behavior, one-day-old gravid adult females are the dominant dispersers (Smitley and Kennedy 1985; Collins and Margolies 1991; Li and Margolies 1993a). Adult females developed under crowded conditions reduce their weight to nearly half of those developed under uncrowded conditions, and disperse without feeding (Mitchell 1973).

*Tetranychus urticae* raise forelegs and forebody adopting distinctive orientation before take-off. Both scale insects and phytoseiid mites orient away from the wind source before they exhibit the aerial take-off posture (Washburn and Washburn 1984; Johnson and Croft 1976). In contrast, regardless of the wind source, *T. urticae* exhibit an aerial take-off posture facing away from light sources, and most frequently become airborne when facing into the wind (Smitley and Kennedy 1985; Margolies 1987). The aerial take-off posture and orientation of *O. pratensis* are identical to those of *T. urticae* (Margolies 1987). Although the behavior has not been investigated in detail, the Kanzawa spider mite, *Tetranychus kanzawai* Kishida (Acari: Tetranychidae), is also likely to adopt wind-borne dispersal Osakabe (1967).

Although the aerial take-off postures common in many wingless arthropods, orienting away from the wind source lifting their forelegs and forebody higher, may increase drag, *T. urticae* most frequently take off when they exhibit the aerial take-off posture facing to the wind source. This raises the question of whether the aerial take-off posture in spider mites functions to increase drag. The objectives of this study were to clarify: (i) aerodynamic effects of the aerial take-off posture; and (ii) actual aerial take-off behavior in *T. urticae*. We constructed three-dimensional (3D) models of *T. urticae* and performed aerodynamic analyses using computer graphics, and examined whether the aerial take-off posture is advantageous to receive greater force from the wind relative to the normal posture. Then, we examined whether the results of the computer analysis of aerodynamics were true for the actual aerial take-off behavior in spider mites through laboratory experiments and field observations.

## Materials and methods

### Measurement of three dimensional forms

We measured the body (length, width and height) and legs (length and width) in adult *T. urticae* females on photographs taken with a scanning electron microscope (SEM) (3D Real Surface View Microscope VE-8800; Keyence). To maintain mites in their natural shape, we adopted the fixation method for preparing mite specimens for SEM observation developed by Saito and Osakabe (1992). Adult females were dipped into MA80 solution (methanol : acetic acid : distilled water = 2 : 2 : 1) for 10 min and then put on slides to allow the solution evaporate for at least 30 min. The specimens were individually set on the stage of the microscope where photographs could be taken from any direction, giving frontal, rear, dorsal, ventral or side views and observed using the SEM (e.g., Fig. 1a).

From these measurements, we determined the sizes for the 3D model, i.e., 0.55 mm in body length, 0.28 mm in body width, 0.2 mm in thickness (or height) of the idiosoma and 0.3 mm for the length of the first leg (Fig. 1b, c). For the aerial take-off posture, the positions of the first legs in the 3D model were lifted upright with inclination of the raised forebody in the aerial take-off posture (Fig. 1b) based on a video of preliminary wind tunnel observations and a photograph published previously (Smitley and Kennedy 1985).

### Analysis of aerodynamic effects

Aerodynamic effects of the aerial take-off posture and the normal posture in *T. urticae* were analyzed using ANSYS/FLOTRAN (ANSYS), the software for finite element

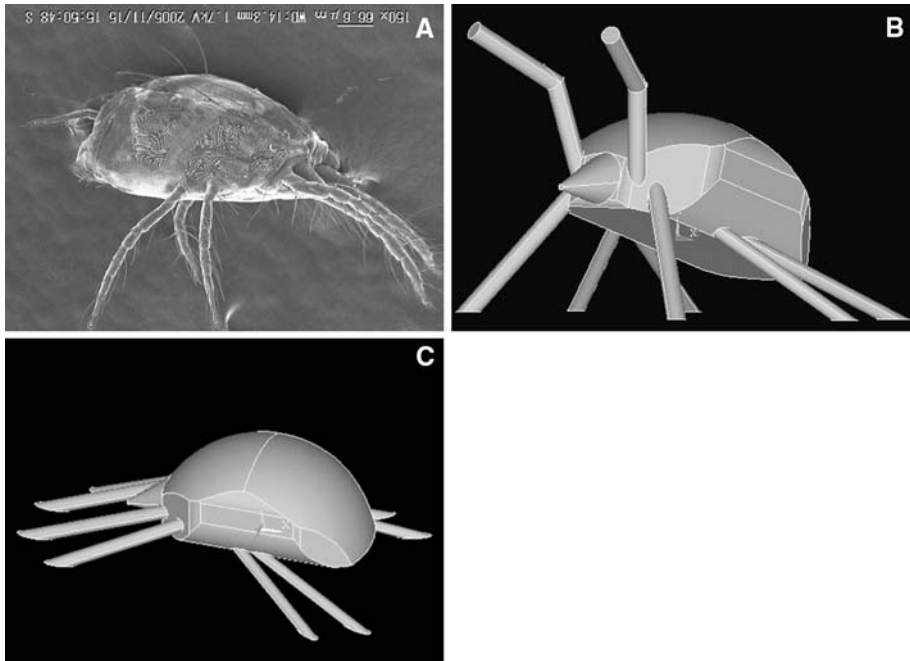


**Fig. 1** Side view of an adult female *T. urticae* by SEM (a), and 3D models with dispersal posture (b) and normal posture (c)

analysis. We constructed finite elements model in which the 3D model described above was in a rectangular solid ( $16 \times 5 \times 6$  mm; Fig. 2a). This is modeled upon a mite on a flat plate with an air flow from the front of it.

#### *Effects of aerial take-off posture on catching wind force*

To evaluate the effects of the aerial take-off behavior on wind drag, we performed fluid dynamics analyses using the 3D models with the aerial take-off posture (Fig. 1b) and the normal posture (Fig. 1c). We numbered the surfaces of the rectangular solid from I to VI as shown in Fig. 2a. The Surface V was the flat plate and the 3D models were attached to the Surface V facing into the wind (Fig. 2a). The surface I was the windward side, and the Surface VI was the leeward. The Surfaces I, II, III, IV and VI were the boundaries just for calculation, and so they were not something like plates in reality. We divided this model into the elements with ANSYS/FLOTTRAN automatic element breakdown function. We set the edge size of the elements 0.01–0.05 mm for the surface of the 3D model, and 2 mm for the rectangular solid surface side, the Surface III side. As a consequence, the elements were smaller in the vicinity of the 3D model and became larger toward the rectangular solid surface. The boundary conditions were as follows:

- Surface I—wind speed: 0.5, 1.0, 1.5, 2.0, or 2.5 m/s (constant air flow),
- Surface II, III, and IV—no friction,
- Surface V, and surface of the 3D model—no flow,
- Surface VI—no pressure.

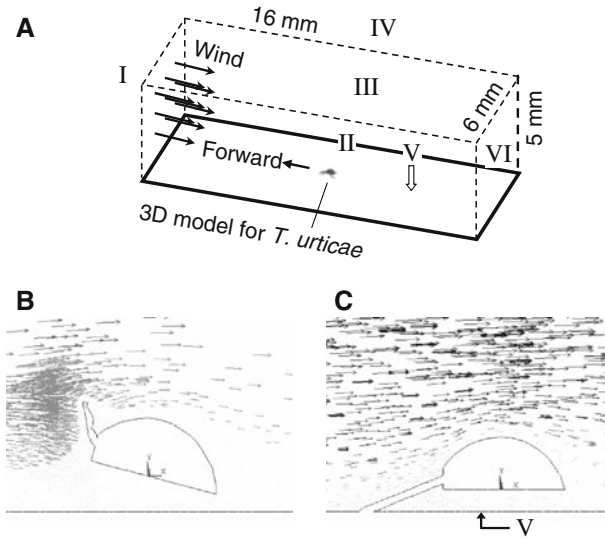


**Fig. 2** Analytical model for aerodynamic analysis (a) and sectional display of air current around models with dispersal posture (b) and normal posture (c) with a wind speed of 1.5 m/s

In the analyses, we assumed conditions of laminar flow, insulation, incompressibility, and steady flow. Initialization temperature was set at 28°C. We confirmed convergence of the results after 300 iterations by using the function of ANSYS/FLOTRAN.

Direction of the friction stress on a given position was determined from air currents around the 3D models (Fig. 2b, c). From these results, we computed the forces ( $F$ ) acting on the idiosoma and the first legs in the rearward and upward positions by the following procedures.

Given that the 3D model was facing in the direction of the  $x$ -axis, the rearward force of the wind pressure was expressed as

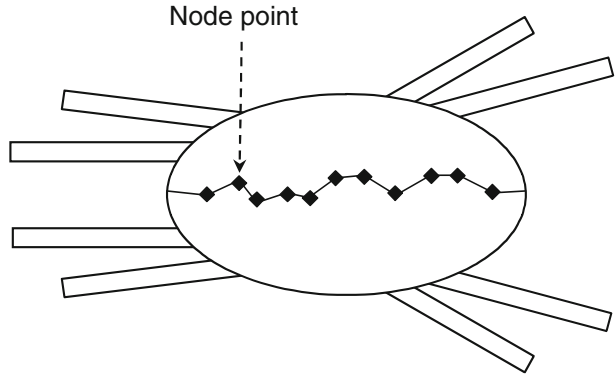
$$F = - \int_S p \mathbf{e}_x \cdot \mathbf{n} dS,$$

where  $p$  is the pressure,  $\mathbf{e}_x$  is the unit vector on the  $x$ -axis,  $\mathbf{n}$  is the unit normal vector on the mite surface,  $S$  is the surface of the 3D model, and  $dS$  is a surface element. We replaced  $p \mathbf{e}_x \cdot \mathbf{n}$  with the average force per unit area ( $P_x$ ) estimated using the following formula:

$$P_x = \frac{\int_l p \mathbf{e}_x \cdot \mathbf{n} dl}{\int_l dl},$$

where  $l$  is a route connecting the node points selected around the median line on the body (Fig. 3), and  $dl$  is a line element. To compute  $P_x$ , the pressure was integrated along  $l$  using FLOTRAN, and the integrated pressure was divided by the length of  $l$ .  $P_y$ ,  $T_x$ , and  $T_y$  in the following formulas were also compute as the same method as  $P_x$ . Given that the vertical direction of the 3D model was the  $y$ -axis, the upward force of the wind pressure was expressed as

**Fig. 3** The node points selected around the median line on the body of the 3D model of mite for the estimation of the average force per unit area ( $P_x$ ) on the body



$$F = \int_S p\mathbf{e}_y \cdot \mathbf{n}dS,$$

where  $\mathbf{e}_y$  is the unit of vector. We replaced  $p\mathbf{e}_y \cdot \mathbf{n}$  with  $P_y$  calculated as

$$P_y = \frac{\int_l p\mathbf{e}_y \cdot \mathbf{n}dl}{\int_l dl}.$$

The rearward force from the friction stress of winds was expressed as

$$F = - \int_S \mathbf{t} \cdot \mathbf{e}_x dS,$$

where  $\mathbf{t}$  is the friction stress. We replaced  $\mathbf{t} \cdot \mathbf{e}_x$  with  $T_x$  calculated as

$$T_x = \frac{\int_l \mathbf{t} \cdot \mathbf{e}_x dl}{\int_l dl}.$$

The upward force from wind friction stress was expressed as

$$F = \int_S \mathbf{t} \cdot \mathbf{e}_y dS.$$

We replaced  $\mathbf{t} \cdot \mathbf{e}_y$  with  $T_y$  calculated as

$$T_y = \frac{\int_l \mathbf{t} \cdot \mathbf{e}_y dl}{\int_l dl}.$$

Cross-sections of the first legs after element division were approximately square. Accordingly, when we computed the forces operating on the first legs, the parameters  $P_x, P_y, T_x,$  and  $T_y$  were multiplied by a coefficient of  $1/\sqrt{2}$  to correct for bias of the selected nodes.

*Effects of inclined departure surface on resultant force of the wind and weight*

In the field, *T. urticae* move onto vertical surfaces or leaf edges when there is wind, and either face downward or extend the first legs and forebodies out over the leaf edge (Smitley and Kennedy 1985). We computed the resultant forces of weight and of wind (resultant force of the pressure and friction stress), given that the  $x$ - and  $y$ -axes rotated anticlockwise every  $5^\circ$  from  $0^\circ$  to  $140^\circ$  keeping the wind direction from the front (Fig. 4). The motivation to disperse in

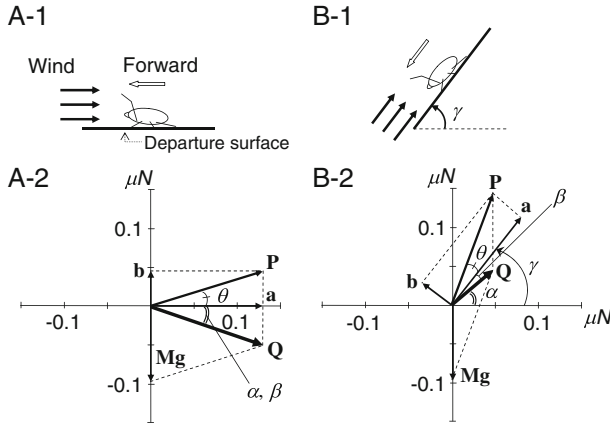


**Fig. 4** Diagrams of 3D model with dispersal posture on a horizontal departure surface (a-1) and the departure surface rotated at an angle of  $\gamma$  (b-1), and horizontal (a-2) and rotated (b-2) coordinate systems with a wind speed of 2.5 m/s and a mass of 10  $\mu\text{g}$ .  $\mathbf{P}$  is the resultant force of rearward (a) and upward forces (b) by the wind, and  $\mathbf{Q}$  is the resultant force of  $\mathbf{P}$  and gravity ( $\mathbf{Mg}$ ).  $\theta$  is the angle of  $\mathbf{P}$  with departure surface,  $\alpha$  is the angle of elevation of  $\mathbf{Q}$ , and  $\beta$  is the angle of elevation of  $\mathbf{Q}$  to the departure surface

*T. urticae* depends on the population density and/or resources (Boykin and Campbell 1984; Smitley and Kennedy 1985; Margolies and Kennedy 1988; Li and Margolies 1993a). Young adult females are the predominant dispersers in spider mites. When they develop under uncrowded conditions, they are estimated to weigh 11–12  $\mu\text{g}$ , while they are somewhat smaller under crowded conditions (5–9  $\mu\text{g}$ ; Mitchell 1973). Therefore, we computed the resultant forces given that the weights of adult females were 5, 7.5, and 10  $\mu\text{g}$ .

Laboratory observation of take-off behavior

We stood a straw vertically in the middle of an area surrounded by lines of sticky material (8 × 8 cm) on a foam polystyrene board with a plastic ball 4 cm in diameter attached to the top of the straw (Fig. 5). The plastic ball was exposed to wind from a small electric fan 20 cm in diameter above which was a cold light. This experimental apparatus was set up in a laboratory at 30°C. The laboratory was also illuminated by fluorescent lights on the ceiling and the wall. All parts of the experimental setup were sufficiently well-lit to allow observation of mite behavior.

We introduced 60 adult females of *T. urticae* onto the plastic ball. The females had developed under crowded conditions on detached kidney bean leaves on water-soaked cotton in Petri dishes at 30°C. The mites were within 3 days after their last molt, and may have been inseminated. The plastic ball was blown by the fan at 1.6 m/s (1.4 m/s behind the plastic ball) for the first 30 min. The wind velocity was then increased to 4 m/s (3.6 m/s behind the plastic ball) for the second 30 min. We observed the distribution and take-off of mites during the second 30-min period, and recorded the number of individuals that took off from each position on the plastic ball (A, B, C, and D) and straw (Fig. 5). Individuals that were blown off accidentally when walking were excluded. At the end of the second 30-min period, we checked the number of individuals orienting in each position. This experiment was replicated four times.

In preliminary experiments, we introduced adult females individually onto the plastic ball blown by the fan at 1.6 m/s. After 2 min, the wind velocity was then set at 1.6 or

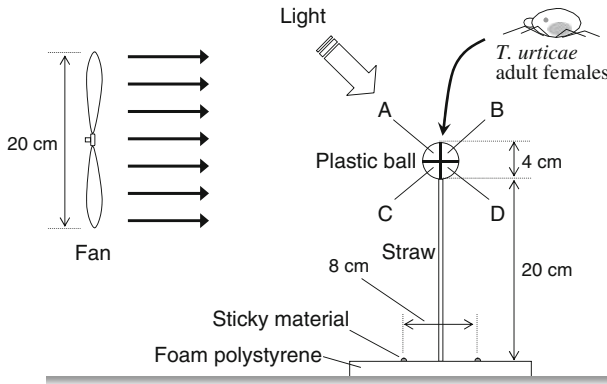


**Fig. 5** Experimental setup for observation of take-off behavior in *T. urticae*

4.0 m/s, and we checked and recorded the behavior of each female every 5 s during 10 min and counted how often they crossed the division between the parts on the plastic ball (Fig. 5). Consequently, the behavior was checked 120 times for each female. We defined the orientation as that the female ceased walking and rested more than for 10 s, and if they rested for 15 s, then we checked their posture whether they lift their forelegs and forebody using a magnifier. As a result, no female was blown off or disappeared during the observation except one female that fell from C part of the plastic ball to a foam polystyrene board. The aerial take-off posture was observed only one time in the whole observation in 1.6 m/s ( $n = 13$ ), while it was observed eight times in 4.0 m/s ( $n = 18$ ; ANOVA,  $P = 0.1176$ ). Orientation was observed more frequently in 4.0 m/s [17 of 18 females oriented;  $38.2 \pm 7.9$  times of observations per female (mean  $\pm$  SE)] than 1.6 m/s (1 of 13 females oriented;  $0.7 \pm 0.7$  times of observations per female; ANOVA,  $P = 0.0004$ ). In contrast, the females walked around more actively in 1.6 m/s than 4.0 m/s; the frequency that the mites crossed the division between the parts on the plastic ball was  $16.2 \pm 2.6$  per females (mean  $\pm$  SE) in 1.6 m/s while  $3.8 \pm 2.6$  in 4.0 m/s (ANOVA,  $P < 0.0001$ ). Although the take-off behavior of *T. urticae* was observed in the wind which velocity was around 1.6 m/s in the previous studies (Smitley and Kennedy 1985; Margolies 1987), results of our preliminary experiments indicated that the wind velocity at 4.0 m/s was more effective in observing the aerial take-off behavior on our setup than 1.6 m/s.

#### Field observation of aerial take-off posture

We observed the aerial take-off behavior of *T. kanzawai* in a tea plantation (100 m<sup>2</sup>), Fuji, Shizuoka Prefecture, Japan (35°11' N, 138°41' E), on May 15, 2005; total daylight was 476 min, the wind direction was west in the early morning and south after 08:00, and the mean wind velocity was 3.06 m/s (Data was obtained from Automated Meteorological Data Acquisition System by the Japan Meteorological Agency). It was the growing season of tea, and the leaves were heavily infested with *T. kanzawai*. We measured the mean wind velocities 40 cm above the tea plant canopy using an anemometer (ISA-80; Shibata Co.) ten times during the period from 15:00 to 16:00. Behavior of *T. kanzawai* was observed at the southern part of tea plants, and individuals exhibiting the aerial take-off posture were photographed. The fact that *T. kanzawai* was dispersing aerially was confirmed by catching wind-dispersing mites using sticky traps (data was not shown).



The aerial take-off behavior of *T. urticae* was observed on carnations in a greenhouse (150 m<sup>2</sup>), Minamiizu, Shizuoka Prefecture, Japan (34°40' N, 138°52' E), during 23–29 October 2006. Then, individuals exhibiting the aerial take-off posture were photographed. It was the harvest season for carnation, and the plants were heavily infested with *T. urticae*.

## Results

### Effects of aerial take-off posture on catching wind force

The aerial take-off posture had a significant obstructing effect on the air current as compared to the normal posture (Fig. 2b, c). The lifted first legs in the aerial take-off posture were effective for receiving greater upward force; the forces were 0.0171  $\mu\text{N}$  in the aerial take-off posture but  $-0.0027 \mu\text{N}$  in the normal posture with a wind velocity of 2.5 m/s. In contrast, the raised forebody was effective in receiving greater rearward forces; the forces were 0.1366  $\mu\text{N}$  in the aerial take-off posture and 0.0621  $\mu\text{N}$  in the normal posture with a wind velocity of 2.5 m/s.

Consequently, for both the upward and rearward directions, the aerial take-off posture resulted in greater force than the normal posture under all wind velocities tested (Fig. 6). Regressions of rearward forces ( $a \mu\text{N}$ ) on the aerial take-off posture and the normal posture were

$$a = 0.0172v^2 + 0.0118v \quad (R^2 = 1)$$

and

$$a = 0.0069v^2 + 0.0078v \quad (R^2 = 0.9999),$$

respectively, where  $v$  is the wind velocity (m/s). Upward forces ( $b \mu\text{N}$ ) were

$$b = 0.0059v^2 + 0.0033v \quad (R^2 = 0.9999)$$

and

$$b = 0.0033v^2 - 0.0003v \quad (R^2 = 0.9995).$$

$b$  was greater than  $a$  in both the aerial take-off and normal postures. Even with the aerial take-off posture, upward forces were unlikely to be sufficient to lift *T. urticae* (5–9  $\mu\text{g}$ ; Mitchell 1973).

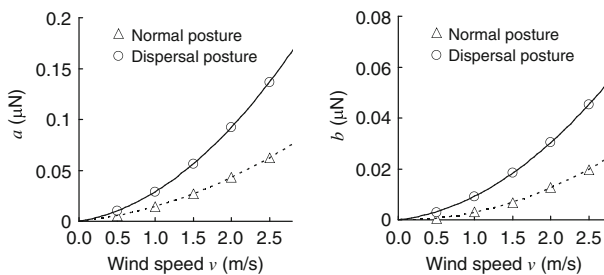


**Fig. 6** Forces by pressure and friction stress operating rearward ( $a$ ) and upward ( $b$ ) on *T. urticae* 3D models with the dispersal posture and normal posture

Effects of inclined departure surfaces on resultant force of the wind and weight

The resultant force ( $Q \mu\text{N}$ ; see Fig. 4) of the wind forces ( $P \mu\text{N}$ ; resultant force of the forces rearward and upward) and gravity ( $Mg \mu\text{N}$ , where  $M (\mu\text{g})$  and  $g$  are the mass of the mite and the acceleration due to gravity, respectively) increased at higher wind velocities ( $v \text{ m/s}$ ; Fig. 7 upper panels). Weak resultant forces were found in both the aerial take-off posture and the normal posture within the range of 0.5–4.0 m/s in  $v$  and 0–140° in the inclines of departure surface (angle of  $x$ -axis:  $\gamma$ ; see Fig. 4). These minima were the points where  $P$  was balanced with  $Mg$ . Therefore, the values of  $v$  at the minima were obtained from the equations

$$P - Mg = 0,$$

and

$$P = f(v) = \sqrt{a^2 + b^2}.$$

$\gamma$  at the bottom was calculated as

$$\gamma = \frac{\pi}{2} - \theta,$$

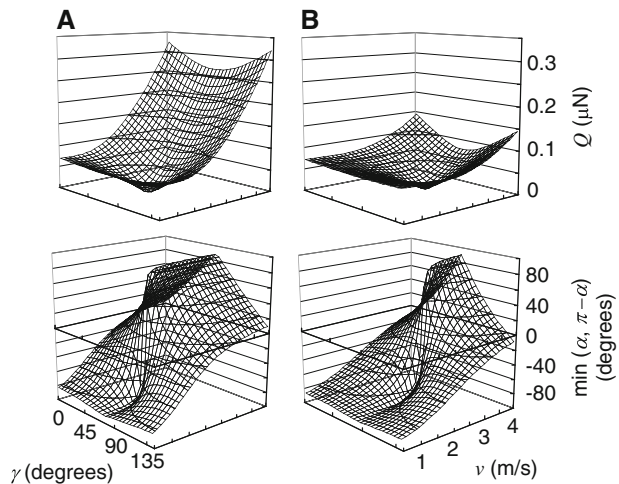
where  $\theta$  is the angle of  $P$  with the departure surface,

$$\theta = \arctan\left(\frac{b}{a}\right)$$

(see Fig. 4).

Given an  $M$  of 7.5  $\mu\text{g}$ ,  $\gamma$  and  $v$  at the bottom were 72.00° and 1.7 m/s in the aerial take-off posture and 72.02° and 2.7 m/s in the normal posture, respectively (Fig. 7, upper panels); when  $M$  was 10  $\mu\text{g}$ , these values were 71.90° and 2.0 m/s in the aerial take-off postures and 71.14° and 3.1 m/s in the normal posture, respectively; and for 5  $\mu\text{g}$  they were 72.17° and 1.3 m/s and 73.42° and 2.1 m/s, respectively. In contrast, the angle of elevation of  $Q$  against the level [ $\alpha$  (or  $\pi - \alpha$ ); see Fig. 4] peaked at  $\gamma$  when  $v$  was greater than those

**Fig. 7** Effects of incline of the departure surface ( $\gamma$ ) and wind speed ( $v$ ) on resultant forces ( $Q \mu\text{N}$ ) of  $\mathbf{P}$  and  $\mathbf{Mg}$  (upper panels) operating on *T. urticae* 3D models (7.5  $\mu\text{g}$ ) in the dispersal posture (a), normal posture (b), and the angle of elevation of  $\mathbf{Q}$  ( $\alpha$ , lower panels). Given that the model faced left on the original, the  $x$ -axis was rotated anticlockwise every 5° from 0° to 140°



at the bottom of  $Q$  (Fig. 7, lower panels). When  $v$  was smaller,  $\alpha$  (or  $\pi - \alpha$ ) became negative with no relation to  $\gamma$ .

Values of  $Q$  acting on the aerial take-off posture were greater than those on the normal posture, and the difference increased with increases in  $v$  (Fig. 8, upper panels). When  $v$  was 2 m/s, only when the model exhibited aerial take-off posture and its weight was given as 5  $\mu\text{g}$ ,  $\alpha$  (or  $\pi - \alpha$ ) was positive in the range of  $\gamma$  from 15° to 130° (Fig. 8, middle panels). In this case, when  $\gamma$  was greater than 55°, the angles of elevation of  $Q$  against the departure surface ( $\beta$ ; see Fig. 4) were positive (Fig. 8, lower panels).  $\beta$  increased sigmoidally with  $\gamma$ . In contrast,  $\alpha$  (or  $\pi - \alpha$ ) decreased with  $\gamma$ , which was greater than the angle at the bottom of  $Q$  mentioned above, while  $Q$  increased.

For aerial take-off, both  $\alpha$  (or  $\pi - \alpha$ ) and  $\beta$  should be positive. Such conditions became narrow with decreasing  $v$  and increasing  $Mg$ . To evaluate the efficacy of  $\gamma$ , we assumed the parabolic motion of aerially dispersing spider mites, and estimated  $\gamma$  values that provided the longest horizontal arrival distance ( $\gamma_{\text{dmax}}$ ) by calculating inflection points of the resulting distances. We assumed that the initial speed ( $V_0$ ) was

$$V_0 = \frac{Q \cdot \Delta t}{M \times 10^{-3}},$$

where  $\Delta t$  is the time to receive the wind force before take-off. The horizontal arrival distance,  $d$ , was given by the common formula

$$d = \frac{V_0^2}{g} \sin 2\alpha,$$

or

$$d = \frac{V_0^2}{g} \sin 2(\pi - \alpha),$$

when  $\gamma$  was larger than the angle at the bottom of  $Q$  mentioned above. According to the cosine theorem,  $\alpha$  was given by

$$\alpha = \arccos \left\{ \frac{P \cos(\theta + \gamma)}{Q} \right\},$$

and  $Q$  by

$$Q = \sqrt{P^2 + (Mg)^2 - 2MgP \cos \left\{ \frac{\pi}{2} - (\theta + \gamma) \right\}}.$$

Therefore, the formula of the horizontal arrival distance was transformed to

$$d = \frac{2 \cdot \Delta t^2 \cdot P}{g \cdot (M \times 10^{-3})^2} \cdot \cos(\theta + \gamma) \cdot |Mg - P \sin(\theta + \gamma)|.$$

when  $\gamma$  ranged from 0 to the angle at the bottom of  $Q$ , and

$$d = - \frac{2 \cdot \Delta t^2 \cdot P}{g \cdot (M \times 10^{-3})^2} \cdot \cos(\theta + \gamma) \cdot |Mg - P \sin(\theta + \gamma)|,$$

when  $\gamma$  ranged from the angle at the bottom of  $Q$  to 140°.  $\gamma_{\text{dmax}}$  was provided as the solution of the equation

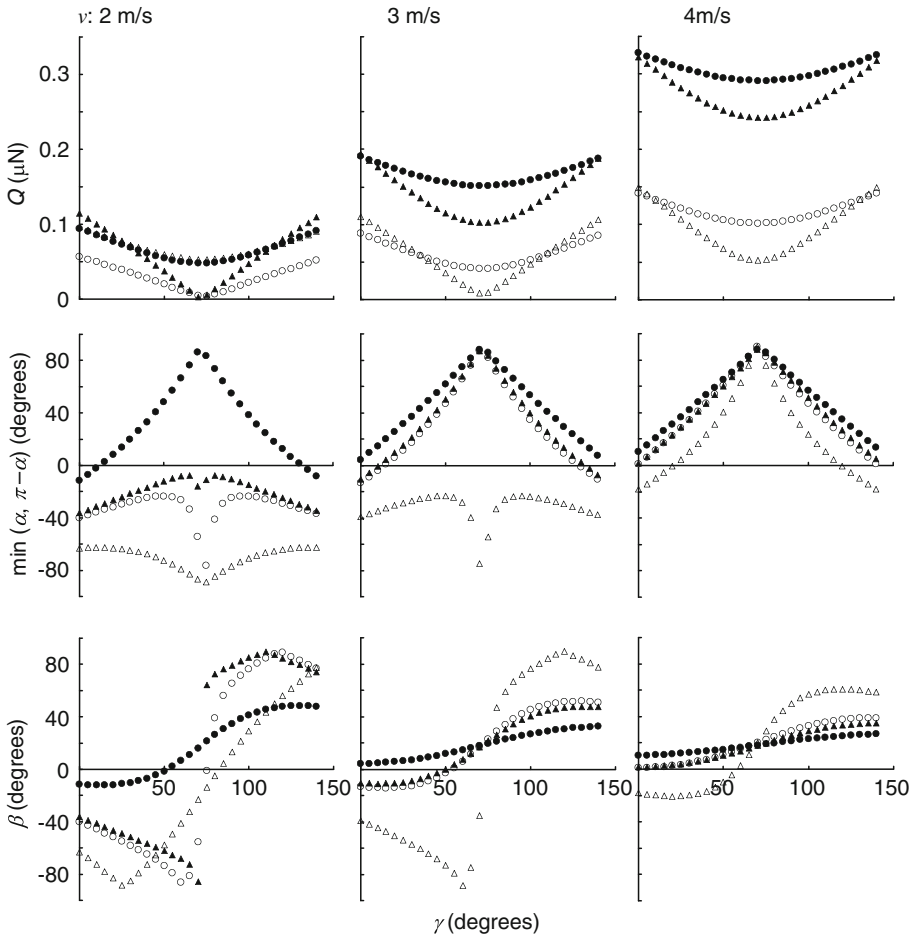


**Fig. 8** Resultant forces ( $Q$   $\mu\text{N}$ ) of  $\mathbf{P}$  and  $\mathbf{Mg}$  (upper panels), angles of elevation ( $\alpha$ , middle panels), and angles from the departure surface ( $\beta$ , lower panels). Solid circles and triangles indicate the results for the dispersal posture, while open circles and triangles indicate the results for the normal posture with masses of 5 and 10  $\mu\text{g}$ , respectively

$$\frac{\partial d}{\partial \gamma} = 0,$$

which was eventually given as

$$\gamma = k\pi + (-1)^k \arcsin\left(\frac{Mg \pm \sqrt{M^2g^2 + 8P^2}}{4P}\right) - \theta,$$

where  $k$  is a positive integer. However, the formula

$$\gamma = k\pi + (-1)^k \arcsin\left(\frac{Mg - \sqrt{M^2g^2 + 8P^2}}{4P}\right) - \theta$$

gave values of  $\gamma$  that were less than  $0^\circ$  and greater than  $180^\circ$ , which were beyond the assumed range from  $0^\circ$  to  $140^\circ$ . Consequently,  $\gamma_{\text{dmax}}$  was given by the formula,

$$\gamma_{\text{dmax}} = k\pi + (-1)^k \arcsin\left(\frac{Mg + \sqrt{M^2g^2 + 8P^2}}{4P}\right) - \theta.$$

Within the extent from  $0^\circ$  to  $140^\circ$  in  $\gamma$ , the longest horizontal arrival distance in each  $v$  and  $M$  was equally provided at the two values of  $\gamma_{\text{dmax}}$ , which were within the ranges of  $29.6\text{--}52.7^\circ$  ( $k = 0$ ) and  $91.4\text{--}113.5^\circ$  ( $k = 1$ ; Table 1). However,  $\beta$  values at the  $\gamma_{\text{dmax}}$  obtained with  $k = 0$  ( $29.6\text{--}52.7^\circ$ ) were largely negative, whereas no negative  $\beta$  values were obtained at the  $\gamma_{\text{dmax}}$  with  $k = 1$  ( $91.4\text{--}113.5^\circ$ ; Table 1, Fig. 8).

In practice, wind-borne mites may be exposed to continuous or periodic wind and turbulence. Under such conditions, a mechanistic model, such as Greene and Johnson’s model developed to predict the dispersal of winged seeds (Greene and Johnson 1989), may provide more realistic horizontal arrival distances (Jung and Croft 2001). The assumption of parabolic motion of aerially dispersing spider mites is too simple to allow accurate estimation of the value of  $d$ . Nevertheless, it may be useful to evaluate the relative advantage of  $\gamma$  at the moment of take-off because  $d$  is simply determined by  $Q$  and  $\alpha$  in parabolic motion.

If updrafts are advantageous for catching free streams above the canopy of host plants that may carry the mites to distant places (Smitley and Kennedy 1985), the height that the mites reach after aerial take-off may also be an important factor in their aerial dispersal.

**Table 1** Incline of departure surfaces that provided the greatest horizontal arrival distance ( $\gamma_{\text{dmax}}$ ) calculated under the assumption of parabolic motion of aerial dispersal spider mites

Mass ( $\mu\text{g}$ )	Posture	$\gamma_{\text{dmax}}$ (degrees) for $k = 0^{\text{a}}$ at each wind speed <sup>b</sup>				
		1.5	2	2.5	3	4 (m/s)
5	Dispersal	<b>52.7</b>	<b>39.5</b>	34.6	32.1	29.6
	Normal	–	–	<b>49.0</b>	<b>40.2</b>	32.5
7.5	Dispersal	–	<b>49.0</b>	<b>39.5</b>	35.3	31.3
	Normal	–	–	–	<b>51.4</b>	<b>37.1</b>
10	Dispersal	–	–	<b>45.6</b>	<b>38.8</b>	33.1
	Normal	–	–	–	–	<b>42.6</b>
Mass ( $\mu\text{g}$ )	Posture	$\gamma_{\text{dmax}}$ (degrees) for $k = 1^{\text{a}}$ at each wind speed <sup>b</sup>				
		1.5	2	2.5	3	4 (m/s)
5	Dispersal	91.4	104.3	108.9	111.2	113.5
	Normal	–	–	95.8	102.5	107.5
7.5	Dispersal	–	94.8	104.0	108.1	111.8
	Normal	–	–	–	91.4	102.9
10	Dispersal	–	–	98.0	104.5	110.0
	Normal	–	–	–	–	97.3

<sup>a</sup> Constants in the formula of  $\gamma_{\text{dmax}}$  (see text)

<sup>b</sup> Figures in bold indicate that the angles of elevation of the resultant force against the departure surface ( $\beta$ ) at  $\gamma_{\text{dmax}}$  were negative

Under the assumption of parabolic motion, the vertical arrival distance ( $h$ ) was given by the common formula

$$h = \frac{V_0^2}{2g} \sin^2 \alpha.$$

This formula could be transformed to

$$h = \frac{\Delta t^2}{2g(M \times 10^{-3})^2} \cdot \{Mg - P \sin(\theta + \gamma)\}^2.$$

Values of  $\gamma$  that provided the highest vertically reachable height ( $\gamma_{\text{HMAX}}$ ) were provided as solutions of the equation

$$\frac{\partial h}{\partial \gamma} = \frac{\Delta t^2 P}{g(M \times 10^{-3})^2} \cdot \{P \sin(\theta + \gamma) - Mg\} \cdot \cos(\theta + \gamma) = 0,$$

when

$$\gamma = k\pi + (-1)^k \arcsin\left(\frac{Mg}{P}\right) - \theta$$

and

$$\gamma = \frac{\pi}{2} - \theta.$$

However, the former equation did not give local maximum heights, and corresponded to  $\gamma$  where  $h = 0$ .  $\gamma_{\text{HMAX}}$  was eventually given by the latter equation:

$$\gamma_{\text{HMAX}} = \frac{\pi}{2} - \theta.$$

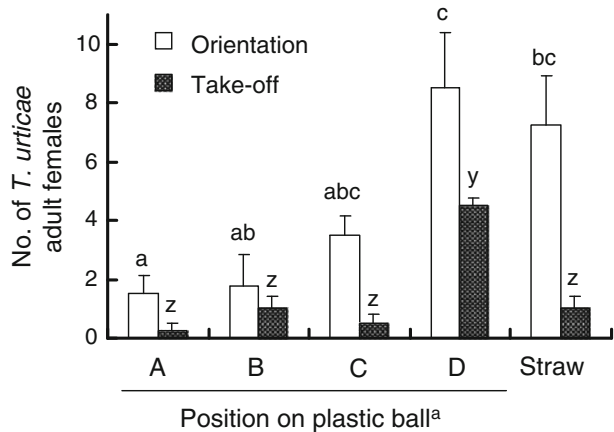
This equation is same as that for the value of  $\gamma$  at the local minimum of  $Q$  described above (see Figs. 7, 8), meaning that the mites reached the highest position when  $P$  was vertically upward. Consequently,  $\gamma_{\text{HMAX}}$  ranged from  $71.5^\circ$  (wind speed: 4 m/s) to  $72.1^\circ$  (1.5 m/s) in the aerial take-off posture, and  $70.0^\circ$  (4 m/s) to  $72.4^\circ$  (2.5 m/s) in the normal posture.

#### Laboratory observation of take-off behavior

During the first 30 min of wind at 1.6 m/s, the adult females actively walked around on the plastic ball and more than half the individuals moved down to the foam polystyrene base. However, after the wind speed was increased to 4 m/s (second 30-min period), most individuals remaining on the plastic ball ceased walking and were oriented downward. The females were oriented in a horizontal arc near the straw on the D part of the plastic ball. However, we did not confirm the posture of oriented individuals whether they were lifting forelegs and forebody in detail because they walked away immediately when we approached with a magnifier. Presumably, the magnifier changed the air stream and disturbed them. Consequently, we counted the number of individuals ceased walking as the frequency of orientation. We excluded individuals that were just walking when they disappeared from the data of “take-off”, but counted individuals that disappeared after the orientation.

During the second 30-min period, the most females took off (disappeared after the orientation) from the leeside of the lower half of the plastic ball (D part, see Fig. 5; Fig. 9). At the end of the second 30-min period, frequency of females oriented was highest at the D

**Fig. 9** Frequencies of orientation and take-off on a plastic ball exposed to wind. <sup>a</sup>See Fig. 3. Different letters on bars of each of orientation and take-off indicate statistically significant differences (Tukey–Kramer method,  $P < 0.05$ )



part (Fig. 9). A significant number of individuals oriented on the straw, but the frequency of take-off from the straw was lower than that from the D part and equivalent to those from parts A, B, and C of the plastic ball (Fig. 9).

#### Field observation of aerial take-off posture

Wind velocity above the sprouts of tea plants where the observation of *T. kanzawai* was performed was  $2.58 \pm 0.70$  m/s (mean  $\pm$  s.d.). Although the take-off behavior has long been unknown, *T. kanzawai* adult females exhibited aerial take-off postures on tea plants as did *T. urticae* on carnation plants (Fig. 10). Mites of both *T. kanzawai* and *T. urticae* walked upward on the plants from feeding sites, thereafter most of them faced downward and exhibited the aerial take-off posture. In some cases, departure sites were locally crowded with the mites exhibiting the aerial take-off posture, suggesting that they selected departure sites based on any condition. During the observation some individuals of *T. kanzawai* exhibiting the aerial take-off posture disappeared from the departure sites (data was not shown). Scarcely any *T. kanzawai* oriented on the upper leaf surfaces, but most were observed oriented on the lower surfaces of young leaves on the sprouts, and some took off from the leaves when there was sufficient wind. In these observations, no threads were found when they exhibited the aerial take-off posture.

#### Discussion

Aerial dispersal of spider mites should affect local and regional population dynamics in prey-predator interaction (Pels and Sabelis 1999; Sabelis et al. 2002) under the meta-population system, and consequently have an effect on the genetic structure of local populations (Tsagkarakou et al. 1997; Osakabe et al. 2005). In this connection, dispersal distance and the fate of wind-borne mites are important factors influencing population structure and dynamics. However, mites of neither group can control landing (Jung and Croft 2000), although morphology and weight affect falling speeds (Jung and Croft 2001). Jung and Croft (2001) reported that the dispersal curves of *T. urticae* and three phytoseiid mite species fit the seed flux model derived by Greene and Johnson (1989). After a period of aerial dispersal, the number of arrivals per unit area is generally expected to decline

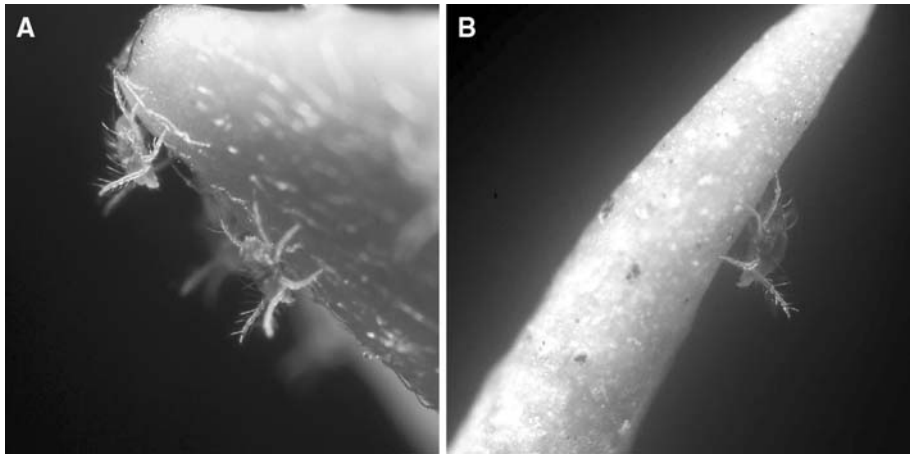


**Fig. 10** Aerial dispersal posture in *Tetranychus kanzawai* on the sprout of a tea plant (a) and in *T. urticae* on a carnation leaf (b)

steeply with increasing distance from the point of departure (Janzen 1970), indicating that aerial dispersal distances of mites are determined stochastically. Although there is a possibility of some in-air behavioral effects (Washburn and Washburn 1984; Jung and Croft 2001), strong natural selection is unlikely to act on in-air behavior of mites, including the control of landing.

In contrast, take-off is likely under the control of the mites as a behavioral response to biological and meteorological conditions. Mite's age and density, host quality, and mating history significantly influence the incidence of aerial take-off behavior in *T. urticae* (Mitchell 1973; Smitley and Kennedy 1988; Collins and Margolies 1991; Li and Margolies 1993a). *Phytoseiulus persimilis* Athias-Henriot, a phytoseiid mite that is a highly specialized predator of spider mites, controls aerial take-off in response to leaf damage caused by *T. urticae* (Sabelis and Afman 1994). Quantitative genetic analysis revealed significant heritability (additive genetic variation) of aerial take-off behavior but no genetic correlations between this behavior and either of two life history traits associated with colonization of new hosts (i.e., fecundity and sex ratio) in *T. urticae*, suggesting that this behavior may be selected directly by nature through underlying morphological or physiological traits (Li and Margolies 1993b, 1994; Margolies 1995).

In previous studies, the aerial take-off behavior of *Tetranychus* was usually investigated on horizontal platforms in laboratory experiments (Smitley and Kennedy 1985; Li and Margolies 1993a). However, aerodynamic analyses with 3D models suggested that the upward forces of winds were insufficient to lift *T. urticae* adult females on such horizontal platforms. In contrast, greater rearward forces acted on the mites. Consequently, based on  $\gamma_{\text{Dmax}}$ , we concluded that for *T. urticae* to take off from inverted departure surfaces an incline of ca. 100–110° was efficient. These results indicated that the undersides rather than upsides of leaves or plant materials were advantageous for *T. urticae* as platforms for aerial take-off. Mites remaining on the upper side of horizontal leaf surfaces move to the leaf edges and extend their first legs and forebodies out over the leaf edge (Smitley and Kennedy 1985). In the laboratory experiments of Smitley and Kennedy (1985), the mites also moved to the edge of the test arena, oriented facing downward, and raised their first legs under conditions appropriate for aerial take-off. Although we do not know the angles



adopted by the mite bodies under such conditions, we estimated that a departure surface incline of around  $70^\circ$  was efficient to reach higher spaces where free air streams may carry the mite long distances. We postulate that such behavior in *T. urticae* has evolved not only to avoid being embedded in the laminar boundary layer formed at the leading edge of the plant substrate, but also to complement the resultant force of wind and gravity to enable the mites to disperse.

Other mites and larvae of scale insects are thought to take off from the upper leaf surface. With regard to the aerial take-off posture, raising legs and body may allow individuals to reach beyond the laminar boundary layer formed by the plant substrate (Washburn and Washburn 1984; Jung 2001): The drag coefficient is higher in this range of Reynolds number (Jung 2001). Taking a thicker boundary layer on the lower leaf surface of a *Populus* leaf (Grace and Wilson 1976), Jung (2001) showed that individuals on the lower leaf surface would have less momentum than those on the upper leaf surface. However, if wingless arthropods take off aurally from the upper surfaces of plant materials, drag sufficient to overcome the force of attachment to the substrate may be required. In contrast, when they take-off from inclined lower surfaces, the influence of the attachment force may be negligible if they release the force holding them in place.

In this study, computations for evaluation of inclines of the departure surface were based on the wind into which *T. urticae* faced, because previous studies showed that wind-borne departure occurred most frequently under such conditions, and the effectiveness of air turbulence on the aerial dispersal response of *T. urticae* has been well documented (Smitley and Kennedy 1985; Margolies 1987). The complicated architecture of plants is likely to cause air turbulence involving updrafts to some extent. As reported by Smitley and Kennedy (1985) light-dependent orientation accounted for the downward-facing aerial take-off posture on host plants in the field, causing dispersal on updrafts leading to greater horizontal displacement. This provides a basis for our assumption. In fact, we confirmed that *T. urticae* adult females oriented preferentially to and took off from inverted positions in the laboratory experiment, and the field observations supported these results. The correspondence of the results of aerodynamic analysis and the empirical evidence demonstrates the rationale of the take-off behavior of *Tetranychus* spider mites.

In addition, aerodynamic analyses revealed the effects of leg position on receiving the wind force, i.e., the lifted forelegs in the aerial take-off posture received greater upward force, while those touching the surface in the normal posture received the forces against the surface. This implies that aerial buoyancy and resulting falling speeds are influenced by in-air postures. Jung and Croft (2001) found no differences in falling speed between active and inactive adult *T. urticae* females. However, the mites in their study were well-fed individuals, which may not be the dominant dispersers. In contrast, aerial dispersal of spider mites occurs under elaborate conditions with a limited range of developmental stages; one-day-old gravid adult females are the dominant dispersers (Smitley and Kennedy 1985; Collins and Margolies 1991; Li and Margolies 1993a), and weights of individuals in the dispersal phase, which developed under crowded conditions, are extremely low (Mitchell 1973). For precise prediction of dispersal distances, effects of in-air postures and weights of the dominant dispersers on their falling speeds must also be re-evaluated and incorporated into appropriate models.

It will be important to determine whether and how the dispersers can control their movement to understand how spider mites inhabiting unstable habitats persist regionally. Moreover, as phytoseiid mites, which are the dominant natural predators of spider mites, are also dispersed by the wind, understanding the role of aerial dispersal of spider mites in

escaping local extinction through predation will help to improve regional integrated pest management (IPM) strategies.

**Acknowledgements** This study was supported by the 21st Century Centers of Excellence Program of Innovative Food and Environmental Studies Pioneered by Entomomimetic Sciences at Kyoto University.

## References

- Bell JR, Bohan DA, Shaw EM, Weyman GS (2005) Ballooning dispersal using silk: world fauna, phylogenies, genetics and models. *Bull Entomol Res* 95:69–114
- Boykin LS, Campbell WV (1984) Wind dispersal of the twospotted spider mite (Acari: Tetranychidae) in North Carolina peanut fields. *Environ Entomol* 13:221–227
- Brandenburg RL, Kennedy GG (1982) Intercrop relationships and spider mite dispersal in a corn peanut agro-ecosystem. *Entomol Exp Appl* 32:269–276
- Collins RD, Margolies DC (1991) Possible ecological consequences of heterospecific mating behavior in two tetranychid mites. *Exp Appl Acarol* 13:97–105
- Croft BA, Jung C (2001) Phytoseiid dispersal at plant to regional levels: a review with emphasis on management of *Neoseiulus fallacis* in diverse agroecosystems. *Exp Appl Acarol* 25:763–784
- Das GM (1959) Bionomics of the tea red spider, *Oligonychus coffeae* (Nietner). *Bull Entomol Res* 50:265–274
- De Angelis JD, Larson KC, Berry RE, Krantz GW (1982) Effects of spider mite injury on transpiration and leaf water status in peppermint. *Environ Entomol* 11:975–978
- Duffner K, Schruft G, Guggenheim R (2001) Passive dispersal of the grape rust mite *Calepitrimerus vitis* Nalepa 1905 (Acari, Eriophyoidea) in vineyards. *J Pest Sci* 74:1–6
- Fleschner CA, Badgley ME, Ricker DW, Hall JC (1956) Air drift of spider mites. *J Econ Entomol* 49:624–627
- Grace J, Wilson J (1976) The boundary layer over a *Populus* leaf. *J Exp Bot* 27:231–241
- Grafton-Cardwell EE, Granett J, Normington SM (1991) Influence of dispersal from almonds on the population dynamics and acaricide resistance frequencies of spider mites infesting neighboring cotton. *Exp Appl Acarol* 10:187–212
- Greene DF, Johnson EA (1989) A model of wind dispersal of winged or plumed seeds. *Ecology* 70:339–347
- Gullan PJ, Kosztarab M (1997) Adaptations in scale insects. *Ann Rev Entomol* 42:23–50
- Hoy MA (1982) Aerial dispersal and field efficacy of a genetically improved strain of the spider mite predator *Metaseiulus occidentalis*. *Entomol Exp Appl* 32:205–212
- Hussey NW, Parr WJ (1963) Dispersal of the glasshouse red spider mite *Tetranychus urticae* Koch (Acarina, Tetranychidae). *Entomol Exp Appl* 6:207–214
- Janzen DH (1970) Herbivores and the number of tree species in tropical forests. *Am Nat* 104:501–528
- Johnson DT, Croft BA (1976) Laboratory study of the dispersal behavior of *Amblyseius fallacis* (Acarina: Phytoseiidae). *Ann Entomol Soc Am* 69:1019–1023
- Jung C (2001) Aerodynamic aspects of dispersal take-off behavior among the phytoseiid mites, *Phytoseiulus persimilis*, *Neoseiulus fallacis* and *N. californicus*. *Korean J Appl Entomol* 40:125–129
- Jung C, Croft BA (2000) Survival and plant-prey finding by *Neoseiulus fallacis* (Acari: Phytoseiidae) on soil substrates after aerial dispersal. *Exp Appl Acarol* 24:579–596
- Jung C, Croft BA (2001) Aerial dispersal of phytoseiid mites (Acari: Phytoseiidae): estimating falling speed and dispersal distance of adult females. *Oikos* 94:182–190
- Lawson DS, Nyrop JP, Dennehy TJ (1996) Aerial dispersal of European red mites (Acari: Tetranychidae) in commercial apple orchards. *Exp Appl Acarol* 20:193–202
- Li J, Margolies DC (1993a) Effects of mite age, mite density, and host quality on aerial dispersal behavior in the twospotted spider mite. *Entomol Exp Appl* 68:79–86
- Li J, Margolies DC (1993b) Quantitative genetics of aerial dispersal behaviour and life-history traits in *Tetranychus urticae*. *Heredity* 70:544–552
- Li J, Margolies DC (1994) Responses to direct and indirect selection on aerial dispersal behaviour in *Tetranychus urticae*. *Heredity* 72:10–22
- Margolies DC (1987) Conditions eliciting aerial dispersal behavior in banks grass mite, *Oligonychus pratensis* (Acari: Tetranychidae). *Environ Entomol* 16:928–932
- Margolies DC (1995) Evidence of selection on spider mite dispersal rates in relation to habitat persistence in agroecosystems. *Entomol Exp Appl* 76:105–108
- Margolies DC, Kennedy GG (1988) Fenvalerate-induced aerial dispersal behavior of the two-spotted spider mite, *Tetranychus urticae* Koch. *Entomol Exp Appl* 46:233–240

- McMurtry JA, Croft BA (1997) Life-styles of phytoseiid mites and their roles in biological control. *Ann Rev Entomol* 42:291–321
- Mitchell R (1973) Growth and population dynamics of a spider mite (*Tetranychus urticae* K., Acarina: Tetranychidae). *Ecology* 54:1349–1355
- Osakabe M (1967) Biological studies on the tea red spider mite, *Tetranychus kanzawai* Kishida, in tea plantation. *Bull Tea Res Stn* 4:1–156
- Osakabe Mh, Goka K, Toda S, Shintaku T, Amano H (2005) Significance of habitat type for the genetic population structure of *Panonychus citri* (Acari: Tetranychidae). *Exp Appl Acarol* 36:25–40
- Pels B, Sabelis MW (1999) Local dynamics, overexploitation and predator dispersal in an acarine predator-prey system. *Oikos* 86:573–583
- Sabelis MW, Afman BP (1994) Synomone-induced suppression of take-off in the phytoseiid mite *Phytoseiulus persimilis* Athias-Henriot. *Exp Appl Acarol* 18:711–721
- Sabelis MW, van Baalen M, Pels B, Egas M, Janssen A (2002) Evolution of exploitation and defense in tritrophic interactions. In Dieckmann U, Metz JAJ, Sabelis MW, Sigmund K (eds) *Adaptive dynamics of infectious diseases: in pursuit of virulence management*. Cambridge University Press, Cambridge, pp 297–321
- Saito Y (1983) The concept of “life types” in Tetranychinae. An attempt to classify the spinning behavior of Tetranychinae. *Acarologia* 24:377–391
- Saito Y, Osakabe Mh (1992) A new fixation method for preparing mite specimens for optical and SEM microscopic observations. *Appl Entomol Zool* 27:427–436
- Sances FV, Wyman JA, Ting IP (1979) Physiological responses to spider mite infestations on strawberries. *Environ Entomol* 8:711–714
- Smitley DR, Kennedy GG (1985) Photo-oriented aerial-dispersal behavior of *Tetranychus urticae* (Acari: Tetranychidae) enhances escape from the leaf surface. *Ann Entomol Soc Am* 78:609–614
- Smitley DR, Kennedy GG (1988) Aerial dispersal of the two-spotted spider mite (*Tetranychus urticae*) from field corn. *Exp Appl Acarol* 5:33–46
- Stephens GR, Aylor DE (1978) Aerial dispersal of red pine scale, *Matsucoccus resinosae* (Homoptera: Margarodidae). *Environ Entomol* 7:556–563
- Tsagkarakou A, Navajas M, Lagnel J, Pasteur N (1997) Population structure in the spider mite *Tetranychus urticae* (Acari: Tetranychidae) from Crete based on multiple allozymes. *Heredity* 78:84–92
- Washburn JO, Washburn L (1984) Active aerial dispersal of minute wingless arthropods: exploitation of boundary-layer velocity gradients. *Science* 223:1088–1089